

**Characterizing complex slope channel reservoirs applying  
Extended Elastic Impedance, Saffron gas field, offshore Nile  
Delta, Egypt**

Journal:	<i>The Leading Edge</i>
Manuscript ID	TLE-2020-0046.R1
Manuscript Type:	Technical standalone article (if no special section applies)
Date Submitted by the Author:	n/a
Complete List of Authors:	Othman, Adel; Al-Azhar University, Geology Metwally, Farouk; Helwan university, Geophysics Fathi, Mohamed; Al-Azhar University, Geology Ali, Ahmed; Qarun Petroleum Company
Keywords:	3D, inversion, reservoir characterization, saturation, seismic
Subject Areas:	Reservoir Characterization, Rock Physics
<b>A Revision of the paper has been accepted by TLE and is awaiting production</b>	

**Characterizing complex slope channel reservoirs applying Extended Elastic  
Impedance, Saffron gas field, offshore Nile Delta, Egypt**

Adel A. A. Othman, Geology Department, Al-Azhar University, Nasr City, Cairo, Egypt.

[A3othman2@gmail.com](mailto:A3othman2@gmail.com)

Farouk Ibrahim Metwally, Geology Department, Helwan University.

Mohamed F. M. Ali, Geology Department, Al-Azhar University, Nasr City, Cairo, Egypt.

[Green\\_geophysics@yahoo.com](mailto:Green_geophysics@yahoo.com)

Ahmed Saied Ali, Qarun Petroleum Company, New Maadi, Cairo, Egypt. 1160.

[Aali\\_13@hotmail.com](mailto:Aali_13@hotmail.com)

**A revision of the paper has been accepted by TLE (The Leading Edge) and is  
awaiting production in Volume 40, issue 2**

## **Abstract**

In a complex reservoir with such a significant degree of heterogeneity, it's a demand to characterize the reservoir using different seismic attributes based on the available data within certain time constraints. Pre-stack seismic inversion and Amplitude variation with offset (AVO) are among those techniques which give excellent results in particular for the gas bearing clastic reservoirs delineation because of the remarkable contrast between the latter and the surrounded rocks. However, challenges arise of data shortage in seismic and /or well data may obstacle applying these techniques. Moreover, if the prediction of water saturation ( $S_w$ ) is needed using the seismic data, it represents a serious challenge because of the independent nonlinear relationship between water saturation and seismic attributes and inversion products. Prediction of water saturation is necessary not only for characterizing pay from non-pay reservoirs but for the economics also. Therefore, Extended Elastic Impedance has been performed to produce a 3D volume of water saturation over the reservoir interval then, 3D Sweetness volume was used in order to grasp the geometry of the sand bodies that have been charged with gas in addition to its internal architecture which could illustrate the different stages in the evolution of the Saffron channel system and the sand bodies distribution both vertically and spatially consequently increase the production and decrease the development risk.

## **Introduction**

The Nile Delta of Egypt is one of the classic delta systems in the world, in particular, the offshore part which is turning up quickly, especially after the late discoveries, to be one of the significant gas provinces. The integration of good-quality 3D seismic and well logs data from many successful drilled wells which were either exploratory or development have indicated an obvious multi

subsequent stages of erosion and deposition within the deep-marine slope channels of upper-Pliocene age (Samuel et al., 2003). Saffron gas field occupying the northwestern part in the West Delta Marine (WDDM) concession, 100 km offshore in the deepwater of the current Nile Delta shoreline (Figure 1). It is one of the major Pliocene gas fields in the offshore Nile Delta which discovered in 1998 by BG after drilling the exploratory well saffron-1.

As revealed from seismic and well data, the depositional environment of the Saffron Field is interpreted to be deposited on delta slope as a submarine canyon system occupied by complex largely channelized fill, with multiple phases of re-incision and was probably active over a considerable period. Many detailed studies of the canyon systems geometry, revealed a complex canyon fill using seismic amplitude analysis, core data, wireline logs, and high-resolution formation micro image (Samuel et al., 2003).

The cornerstone of the canyons is major incision surfaces that could be identified from the seismic data. Which helps in defining the cutting of the canyons and canyon geometry. Channels not the same as canyons, the latter are filled with a complex sequence of turbidites which include transgressive sandstones, slumps, crevasse splays, as well as numerous over-bank deposits. The key elements of saffron canyon fill are shown in Figure 2. The term “channel” is used to describe certain confined sand-dominated deposits within each of the canyon complexes. consequently, the saffron canyon contains three stacked and amalgamated channel fill sediments which interpreted as a slope channel deposited in the lowstand system. The three channels were defined as, from younger to older, Channel A, B, E as shown in figure 3.

The Pliocene sand reservoirs were charged by a mixture of thermogenic and biogenic gas from the north, The trapping mechanism is a combination of dip closure to the north and stratigraphic

closures to the southern, eastern and western limits in the form of pinching out and is likely to be top sealed by the overlying non-reservoir mudstones, siltstones, and minor thin-bedded sands.

The reservoir composed of successive sandstone and mudstones arranged in an upward-fining profile. Sand bodies, which formed as a result of deepwater gravity-flow, include laterally amalgamated channels, sinuous channels, channels with frontal splays, and levees. The Saffron channel is interpreted to be the late to early lowstand slope incision (Cross et al., 2009).

The Saffron channel system is oriented NNW-SSE and its width ranges from 5 km to 10 km and approximately 25 km in length. there are almost 40 m of pay gas sand out of 150 m gross thickness of the reservoir, with an average porosity of 25% and an average  $S_w$  of 37%.

As a result of the significant heterogeneity, the aim of this study is to characterize this complex reservoir with such degree of heterogeneity. Therefore, our workflow includes two steps: the first step Applying Extended Elastic impedance to produce a 3D volume of Water saturation to predict the water saturation away from drilled wells. The second included integrating the  $S_w$  cube with the 3D volume of Sweetness attribute in order to determine the geometry of the sand bodies itself which provided the evolution stages of the saffron Channel system during the time.

## **Methodology**

The available data are classified into well logs and pre-stack 3D seismic data. The obtained well logs include Gamma Ray (GR), Resistivity ( $R_t$ ), P-wave velocity ( $V_p$ ), S-wave velocity ( $V_s$ ) and density ( $\rho$ ) logs, in addition to the calculated Petrophysical logs which are water saturation ( $S_w$ ), and shale volume ( $V_{shale}$ ) logs. three wells will be involved in this study, and another one will be used as blind QC well. Figure 4 illustrates an example of our data.

The Workflow for the Extended Elastic Impedance (EEI) is shown in figure 5. The first step is to load and QC input 3D seismic data and water saturation logs, then perform EEI log correlation at each well in order to determine the best chi angle at which we got an optimal correlation of EEI log and the Sw log. The correlation angle performed in the range from -90 to 90. This gives promise of a fast and effective way to relate the EEI inversion results to the reservoir properties such as Water saturation (Whitecomb et al. 2002). Figure 6 shows that the high correlation for Sw is associated with approximately specific Chi for all wells and the average correlation is 80% observed at a chi angle of approximately 28° see figure 6.

Conditioning of the seismic data should be applied carefully in order to give a meaningful result. The misalignment was performed to flatten the seismic event on the prestack data by applying an optimal time shift to all traces followed by offset scaling and filtering. After conditioning, first, we created intercept and gradient volumes. Second, we created a reflectivity volume at the chi angle that obtained previously from well data, applying the following equation:

$$R_s = A \cos x + B \sin x \quad (\text{Whitecomb et al. 2002})$$

Where,

Rs: scaled reflectivity, A: intercept, B: gradient, and  $x$ : the chi angle. Third, we estimated the wavelet from the created reflectivity volume and built an initial model using the EEI logs created at angle 28° in order to invert that volume to get a 3D cube for water saturation property distribution for the reservoir. The full insight for the channel architecture can be resulted by integrating sweetness volume attribute which could help in delineating the reservoir by capturing the lateral changes that recorded in seismic traces whatever structural or stratigraphic changes. Sweetness is a useful attribute for channel detection or other stratigraphic features when those features can be distinguished from a “background” lithology by a combination of instantaneous

frequency and reflection strength. It is derived by dividing reflection strength by the square root of instantaneous frequency (Hart, 2008)

By switching over from Amplitude to frequency domain, to apply spectral Decomposition analysis in order to capture the fine features of the channel in Saffron canyon. After analyzing the seismic spectrum, the dominant frequency was approximately 30 Hz so, we applied the Fast Fourier transform method to decompose the seismic data to three frequencies which were: 14, 30, 54 Hz which will be blended together.

## **Results:**

For QC purposes, we kept one well away in our study in order to use it as a QC well for the results. The blind well is Saffron-Df which lies to the south of the study area. The correlation coefficient between the actual Sw log and the calculated water saturation is 0.71, we compared the results of the 3D water saturation Volume at the blind well location as can be seen in figure 7 where the distribution of the saturation will give the insight to the charged sand bodies. By applying the spectral decomposition on the 3D seismic data, we captured the smaller details for our complex slope channel.

The depositional evolution of the Saffron channels system complex was explained by (Samuel et al, 2003) when the stage I started with the initial erosion of the channel, then deposition of complex amalgamated sand bodies made up of numerous intersecting channels in Stage II (figure 8), followed by the fill of re-incision phase which characterized by stacking of individual thalweg channels in stage III, as seen in (Figure 9), and channels with frontal splays and leveed overbank in stage IV (Figure 10). Finally, the channel system is abandoned during mudstone deposition in stage V (Figure 11).

## Conclusion

Saffron field has a complex largely channelized fill, with multiple phases of re-incision, and was probably active over a considerable period. The Extended Elastic Impedance (EEI) has successfully predicted 3D volume of water saturation which is considered as one of the required elements for reservoir modeling. The EEI workflow was straightforward and non-complicated which starts with identifying the Chi angle which corresponds to water saturation in order to produce reflectivity volume of the property and the last step is to invert the latter volume. The results show a good correlation to the actual saturation which encourage to be applied on the same slope channel systems of clastic reservoirs. Spectral decomposition enhanced the ability to identify the lateral variability of the channel complex as well as shows clearly the evolution of the saffron channel complex system when combined with the water saturation that was blended to the sweetness attribute which, in turn, could facilitate the future development.

## References:

Cross, N. E., A. Cunningham, R. J. Cook, A. Taha, E. Esmaie, and N. El Swidan, 2009, Three-dimensional seismic geomorphology of a deep-water slope-channel system: The Sequoia field, offshore West Nile Delta, Egypt: AAPG Bulletin, **93**, no. 8, 1063–1086, <http://dx.doi.org/10.1306/05040908101>.

Hart, 2008, Channel detection in 3-D seismic data using sweetness, AAPG Bulletin, v. 92, no. 6 (June 2008), pp. 733–742

Mohamed, I. A., O. Shenkar, and H. Mahmoud, 2017, Understanding reservoir heterogeneity through water saturation prediction via neural network — A case study from offshore Nile Delta: The Leading Edge, **36**, no. 4, 298–303, <https://doi.org/10.1190/tle36040298.1>



Samuel, A., B. Kneller, S. Raslan, A. Sharp, and C. Parsons, 2003, Prolific deep-marine slope channels of the Nile Delta, Egypt: AAPG Bulletin, **87**, no. 4, 541–560.

Whitcombe, D., Connolly, P., Reagan, R., Redshaw, T., 2002, Extended elastic impedance for fluid and lithology prediction. Geophysics. 67, No. 1, 63-67, <http://dx.doi.org/10.1190/1.1451337>

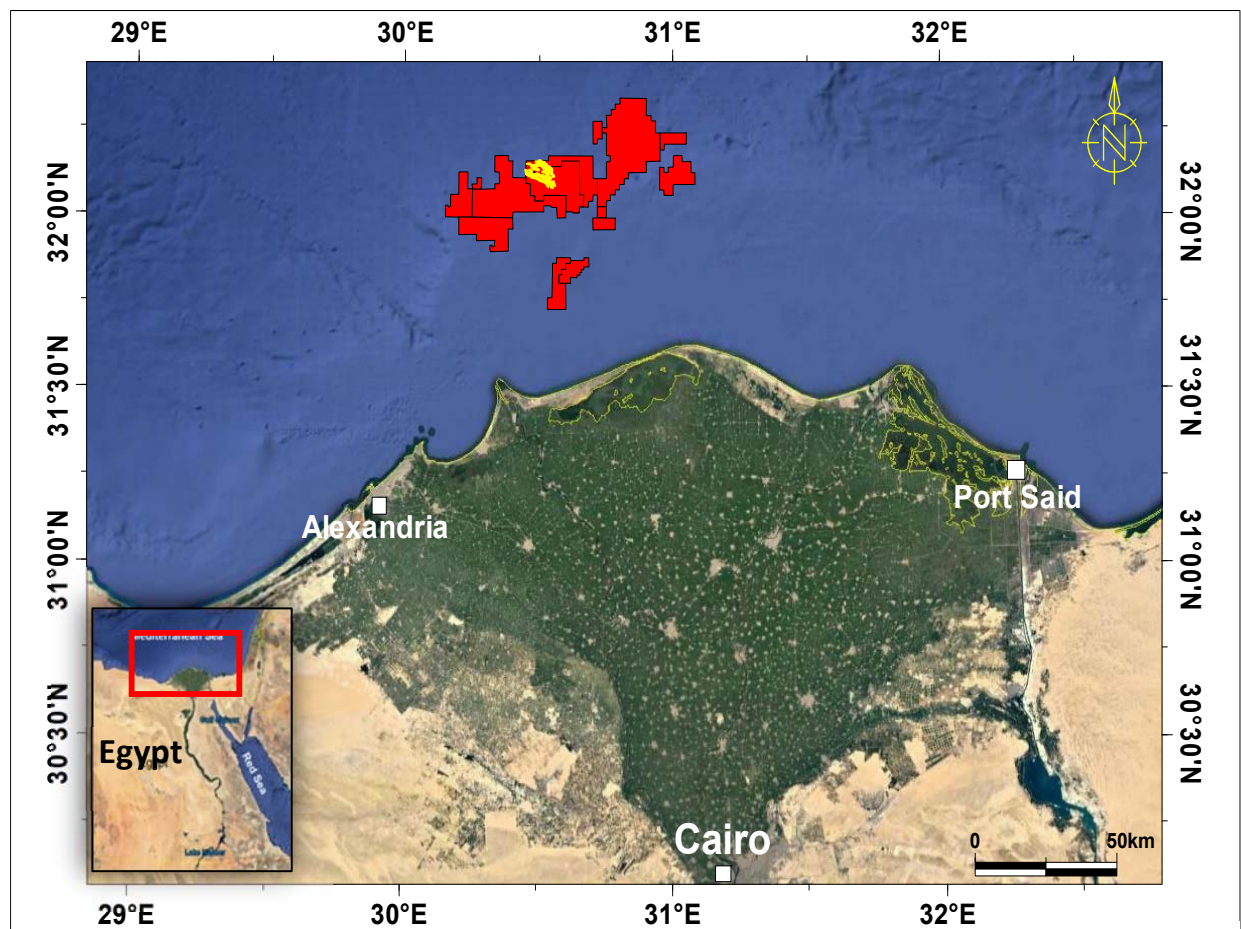


Figure 1. Location map of the Nile Delta of Egypt showing the Saffron field (in yellow) in the West delta deep marine concession WDDM (in red) (modified from Google Earth).

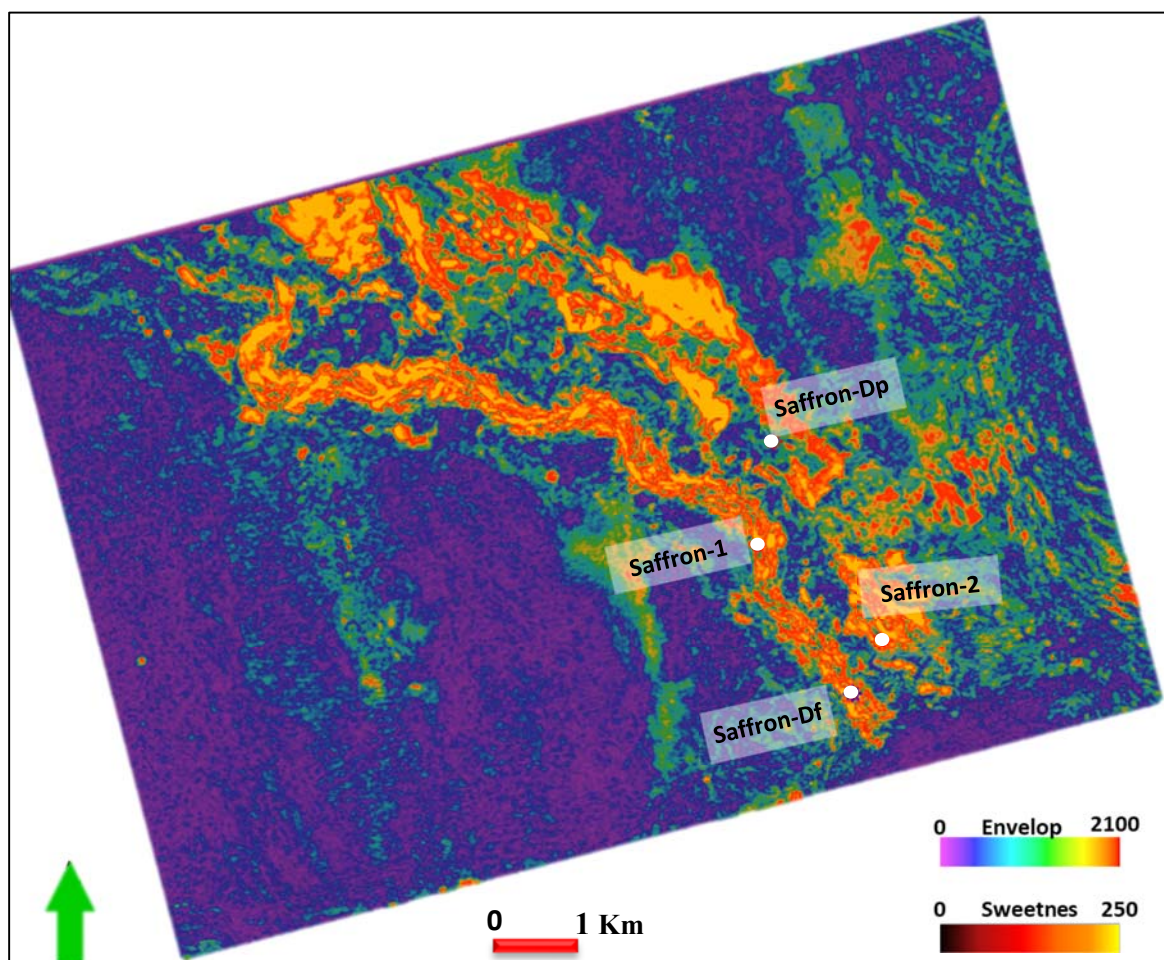


Figure 2. Envelop map for saffron field overlying Sweetness slice extracted 50 ms below the top of the Channel. Four wells have been used in this study.

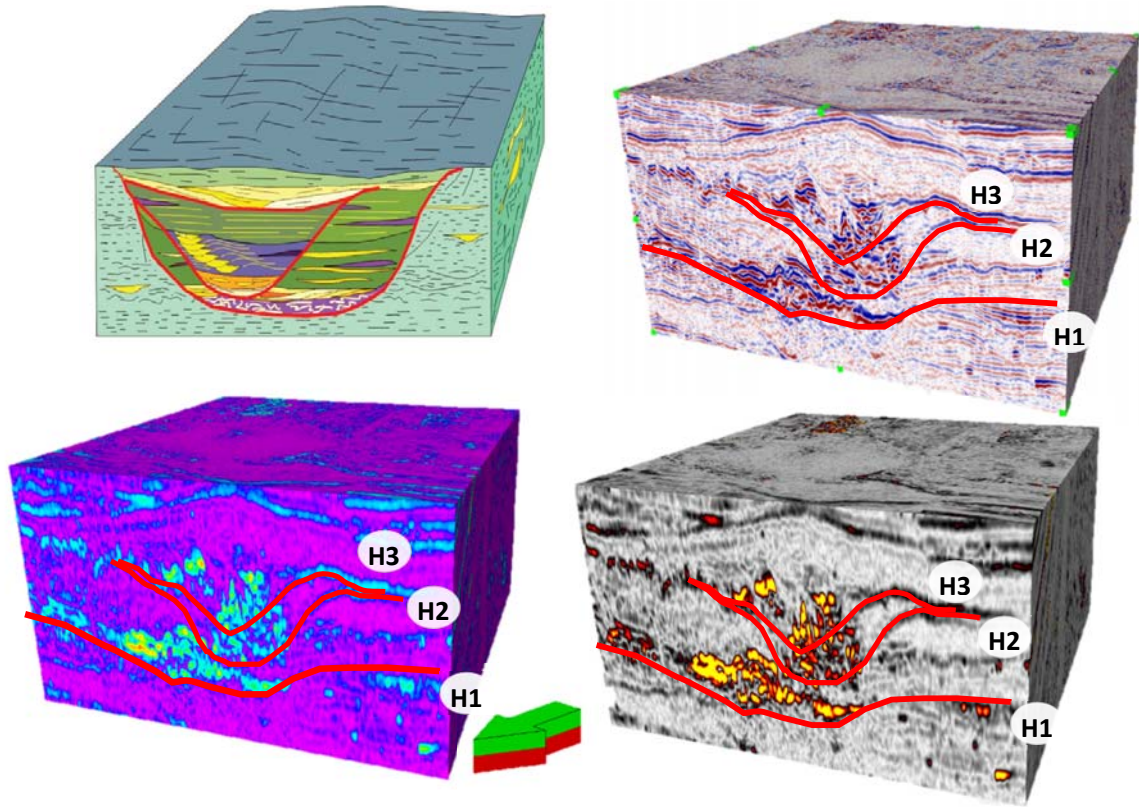


Figure 3. a) Schematic block Diagram for representative canyon complexes (Samuel et al, 2003), b) an actual seismic, c) envelop attribute, and d) sweetness attribute volumes from Saffron Field. Red lines represent incision surfaces cutting through background slope valley deposits where; H1 represents the base of the Saffron slope valley, H2 and H3 represent channel re-incision surfaces.



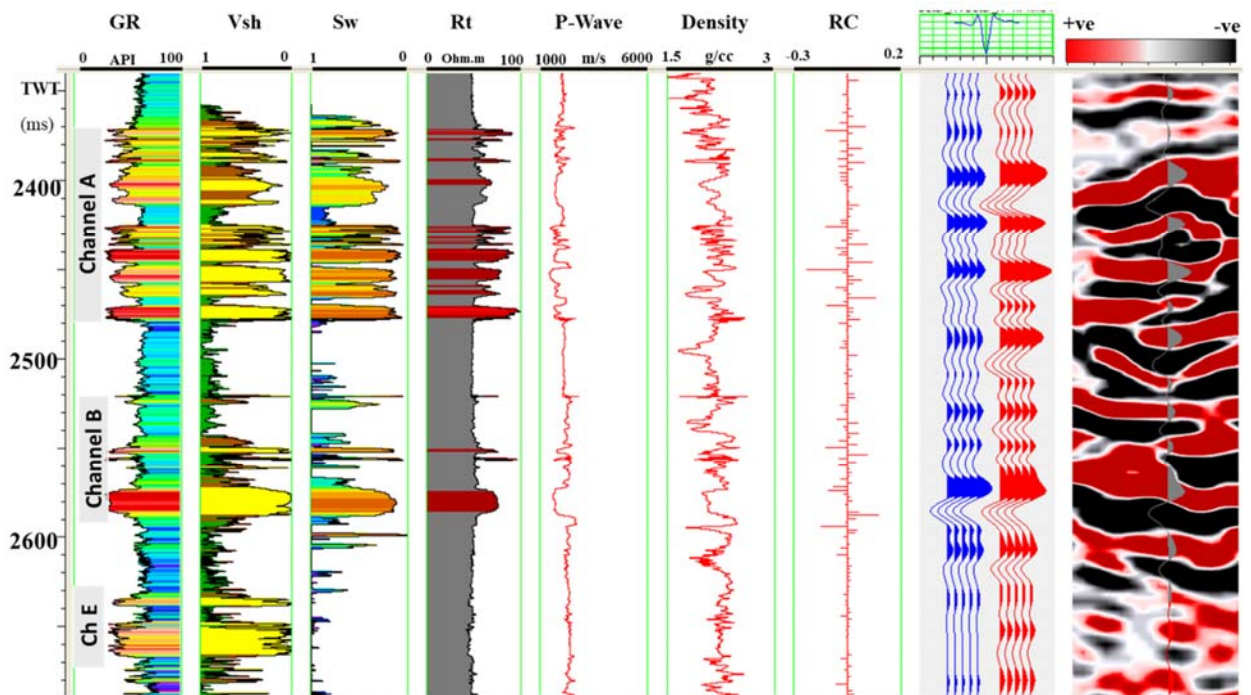


Figure 4. an Example of the available data and the well-to-seismic tie at saffron-1. the well logs from left to right are: Gamma Ray (GR), Shale volume (Vsh), Water saturation (Sw), Deep Resistivity Rt), P-wave, Density, and Reflectivity (RC) respectively.

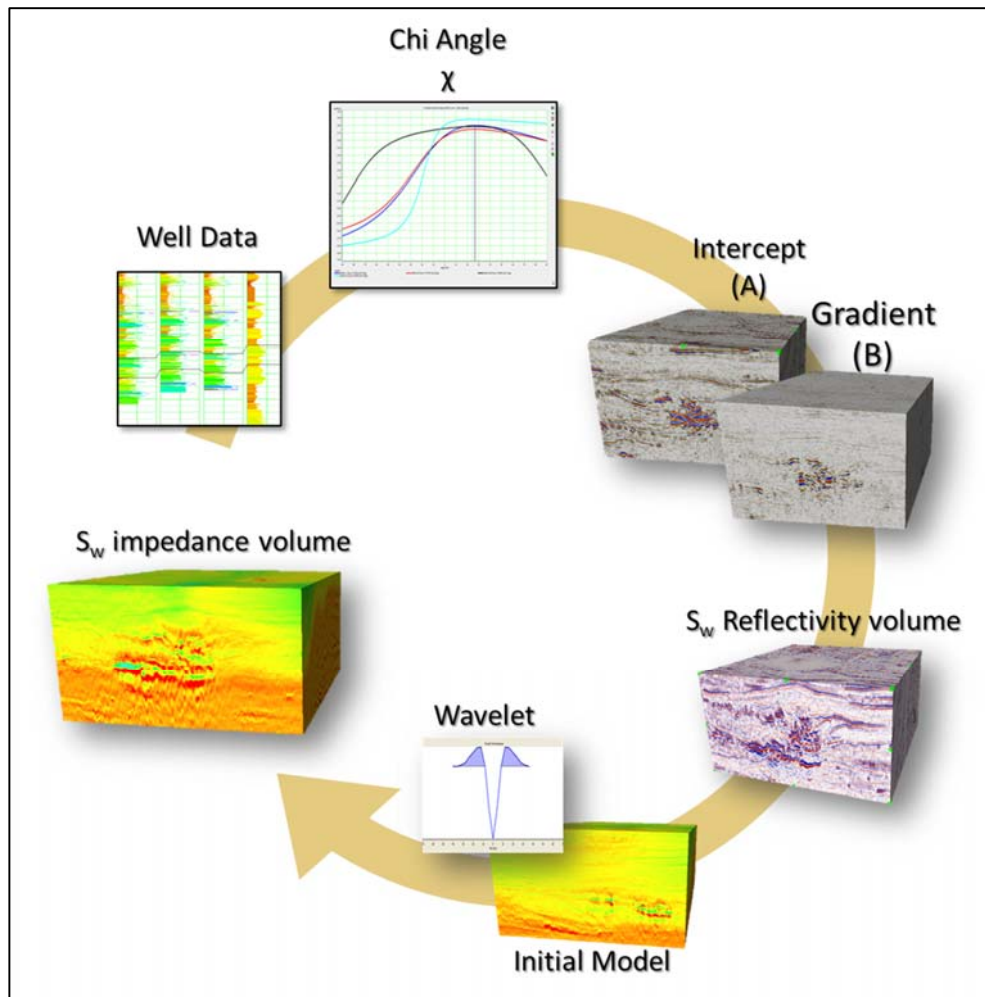


Figure 5. Extended Elastic Impedance (EEI) Workflow

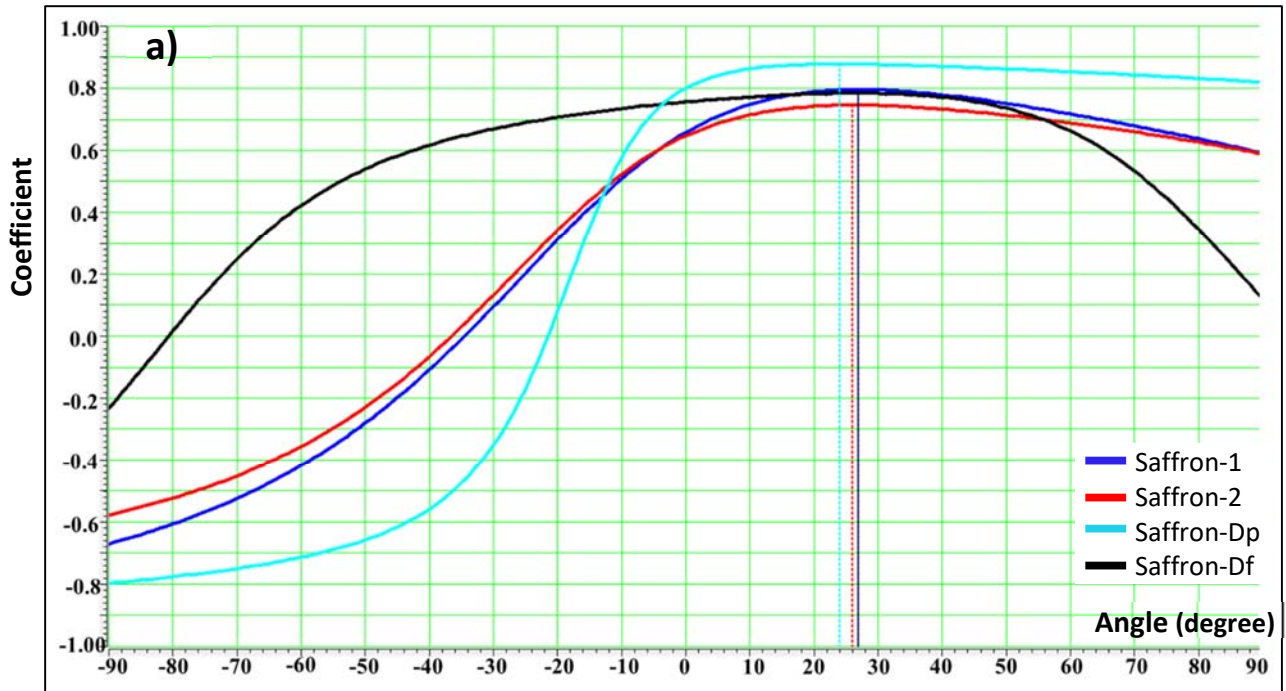
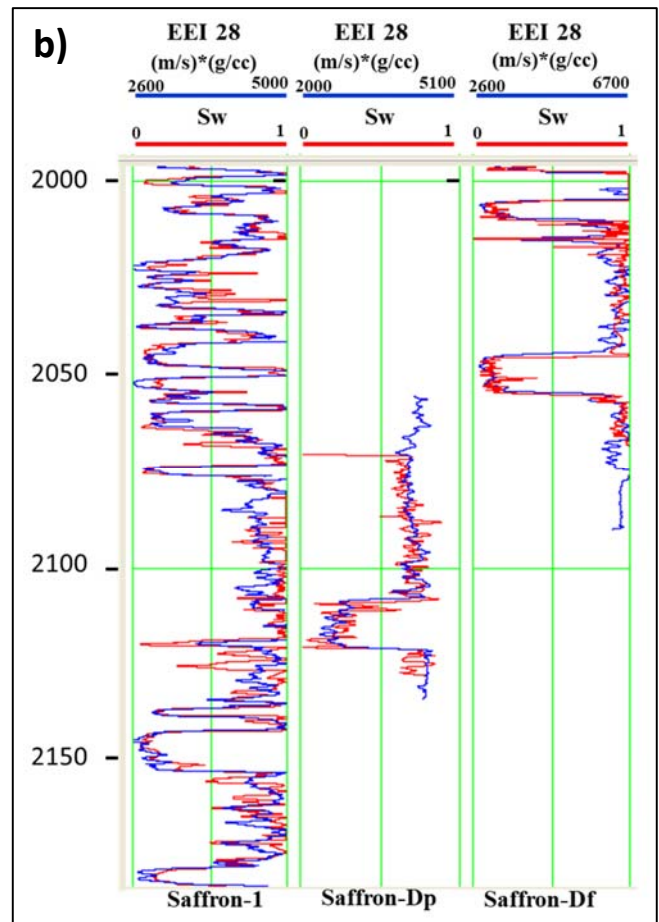


Figure 6 a) illustrates the correlation coefficients between EEI log at 28° and Sw curve for range of values of  $\chi$ , the highest correlation is 88% at Saffron-Dp while the lowest correlation is 72% at Saffron-2 and 80% and 75 % at Saffron-1 and saffron-Df respectively. b) comparing the Sw calculated by the petrophysical analysis (in red) and the Resulted EEI at 28° (in blue) for Saffron-1, saffron-Dp and saffron-Df.



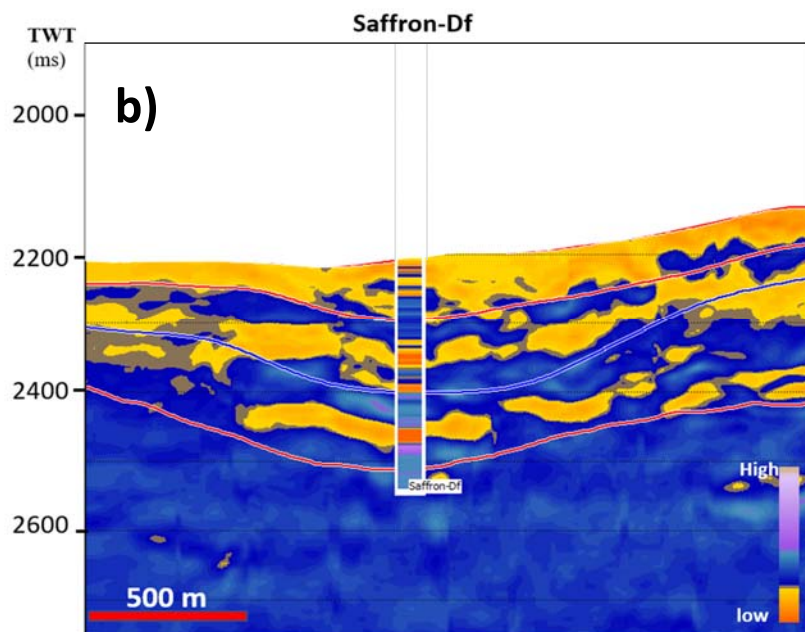
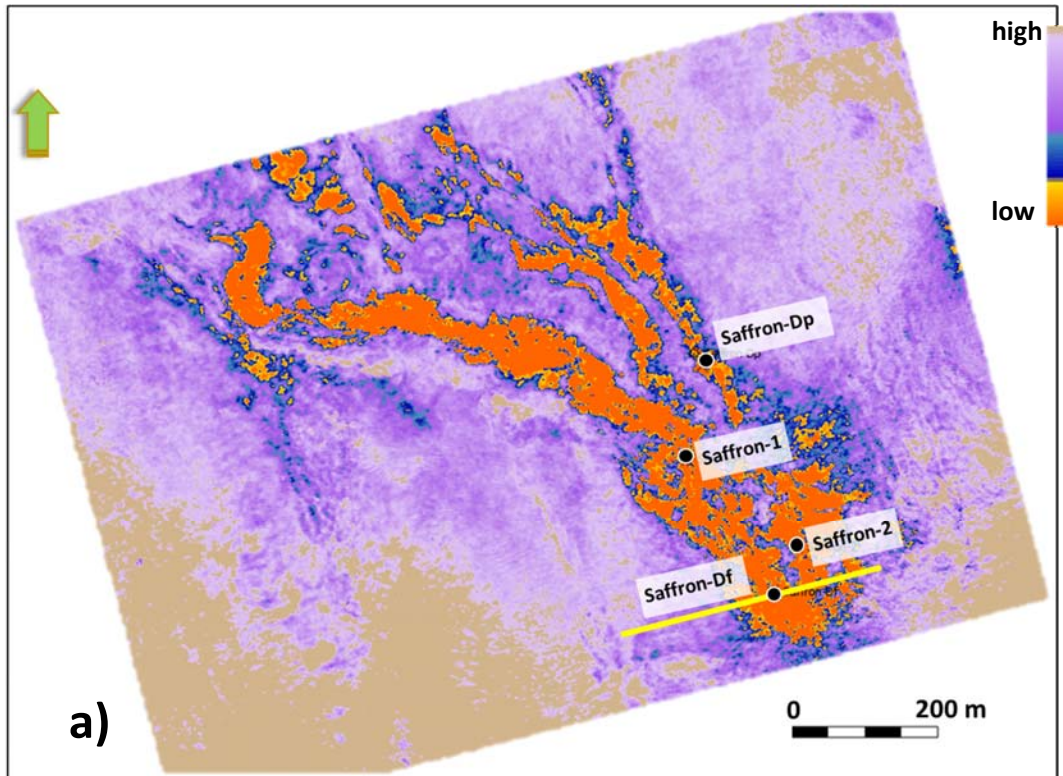


Figure 7. a) Maximum Absolute Amplitude horizon slice from Top of Channel A to the Base of Channel A+15 ms for the EEI 28° volume which illustrates the distribution of the water saturation in the study area. b) Seismic section passing through the resulted Sw volume comparing its results to the calculated Sw log at the blind well.



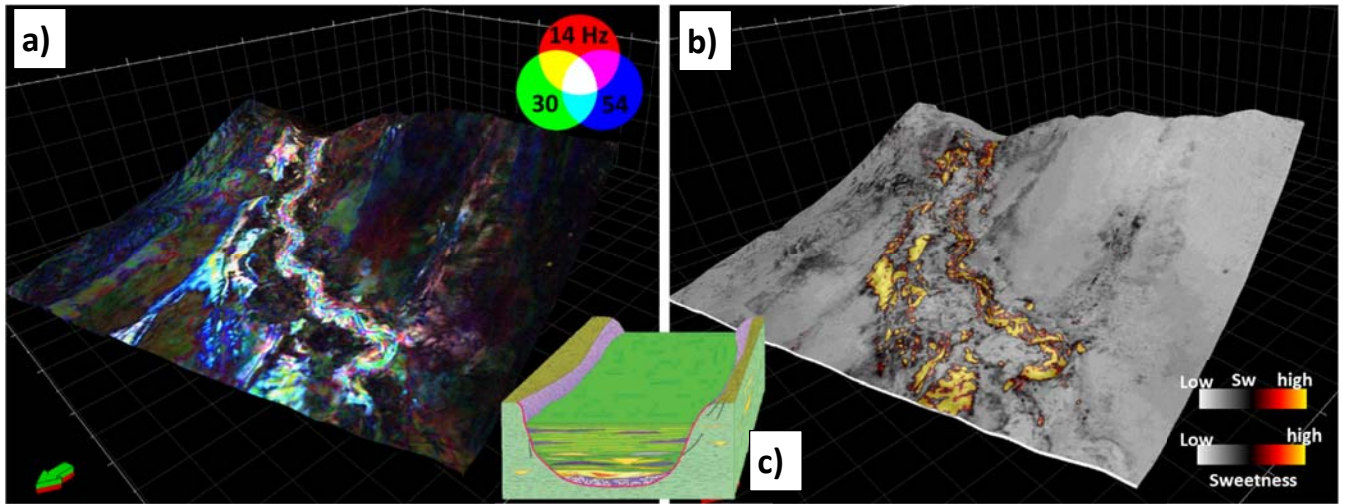


Figure 8. (a) Spectral decomposition map, (b) average Sw map overlays Sweetness slice showing the early stage of the evolution of the saffron channel system (80-100 ms below top channel surface), and (c) a schematic block diagram (from Samuel et al., 2003) describes stage II: the deposition of laterally amalgamated channels.

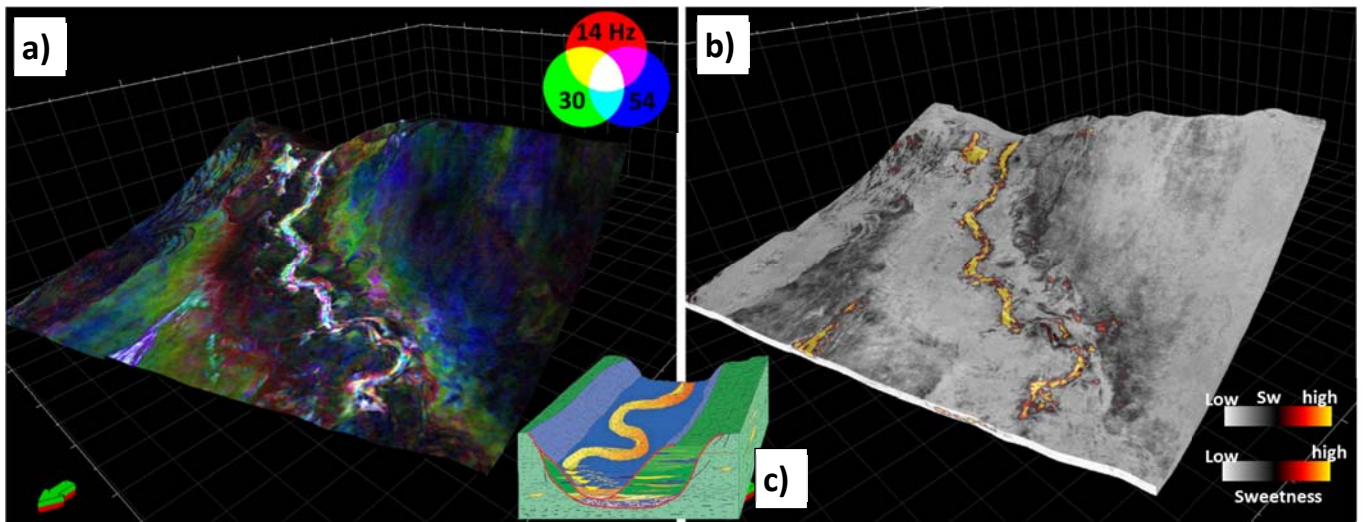


Figure 9. (a) Spectral decomposition map, (b) average Sw map overlays Sweetness slice demonstrating the early stage of the evolution of the saffron channel system (40-80) ms below top channel surface), and (c) a schematic block diagram (from Samuel et al., 2003) describes stage III: the deposition of laterally amalgamated channels.

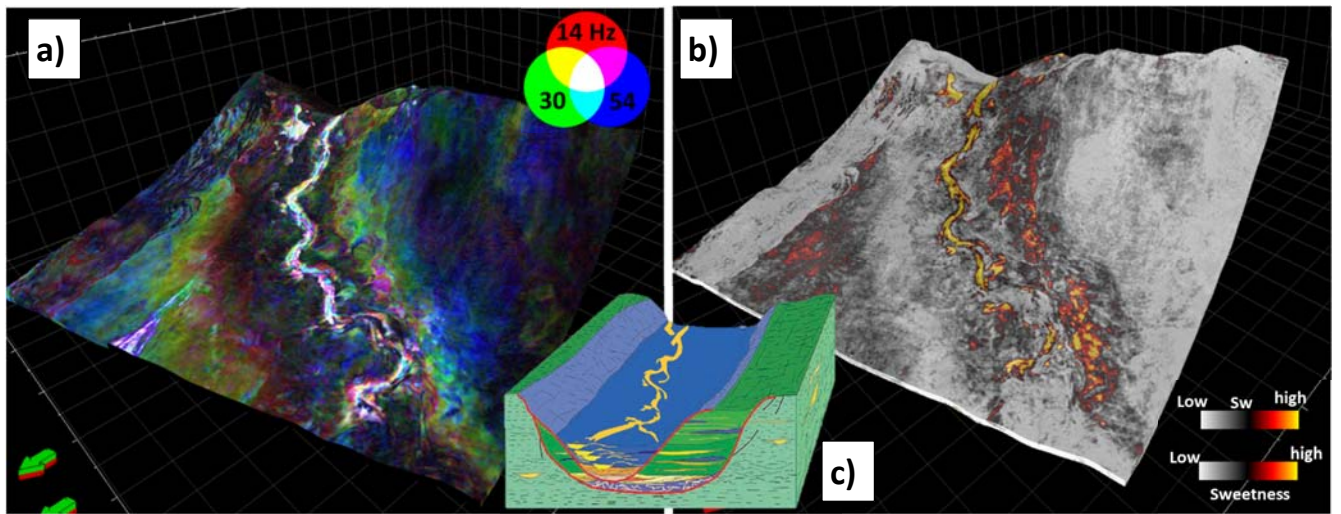


Figure 10. (a) Spectral decomposition map, (b) average Sw map overlays Sweetness slice demonstrating the early stage of the evolution of the saffron channel system (20-40) ms below top channel surface), and (c) a schematic block diagram (modified from Samuel et al., 2003) describes stage III: the deposition of laterally amalgamated channels.

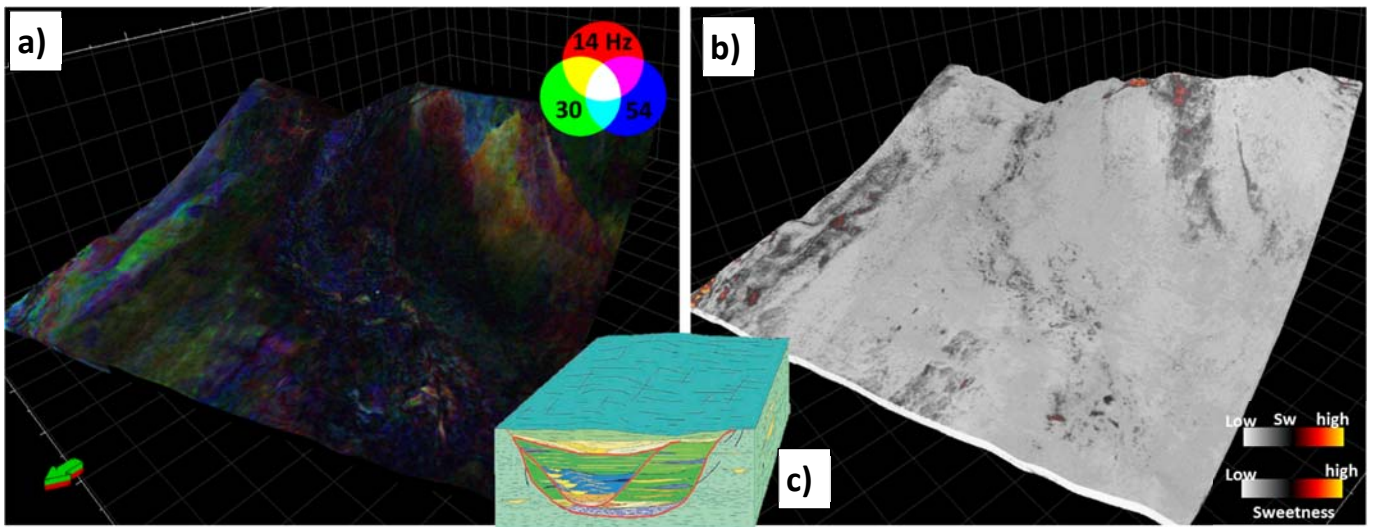


Figure 11. (a) Spectral decomposition map, (b) average Sw map overlays Sweetness slice demonstrating the early stage of the evolution of the saffron channel system 10 ms below top channel surface), and (c) a schematic block diagram (from Samuel et al., 2003) describes stage III: the deposition of laterally amalgamated channels.